Supporting Information

Dense Charge Accumulation in MXene with Hydrate Melt Electrolyte

Kijae Kim,[†] Yasunobu Ando,[‡,§] Akira Sugahara,[†] Seongjae Ko,[†] Yuki Yamada,[†,‡] Minoru Otani,[‡,§] Masashi Okubo,[†,‡] and Atsuo Yamada*[,†,‡]

[†]Department of Chemical System Engineering, School of Engineering, The University of Tokyo, 7-3-1, Hongo, Bunkyo-ku, Tokyo 113-8656, Japan

[‡]Elemental Strategy Initiative for Catalysts & Batteries (ESICB), Kyoto University, Nishikyo-ku, Kyoto 615-8510, Japan

[§]CD-FMat, National Institute of Advanced Industrial Science and Technology (AIST), Umez ono 1-1-1, Tsukuba, Ibaraki 305-8568, Japan

*Corresponding author: yamada@chemsys.t.u-tokyo.ac.jp

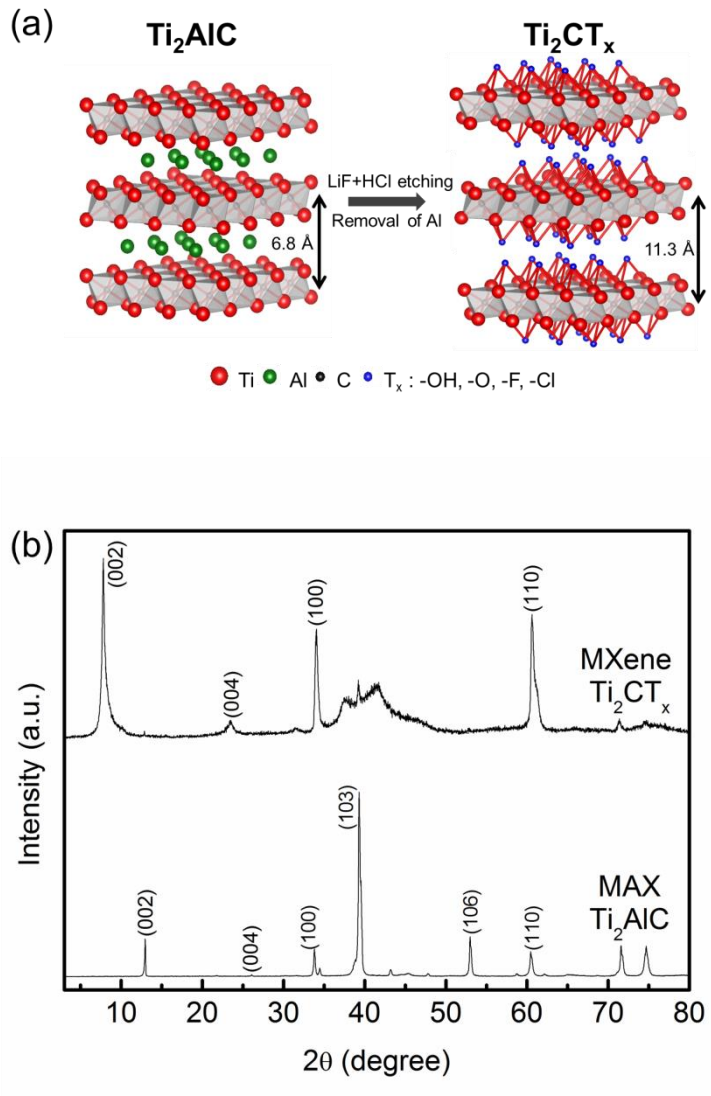

Figure S1. (a) Schematic illustration of the synthesis of Ti_2CT_x. LiF/HCl treatment removes Al layer from Ti_2AlC, and a remaining Ti_2C layer is functionalized by surface termination groups such as -F, -Cl, -OH, or -O. (b) XRD patterns of Ti_2AlC and Ti_2CT_x. The interlayer distance increases after the transformation from Ti_2AlC to Ti_2CT_x due to the attachment of the surface termination groups.

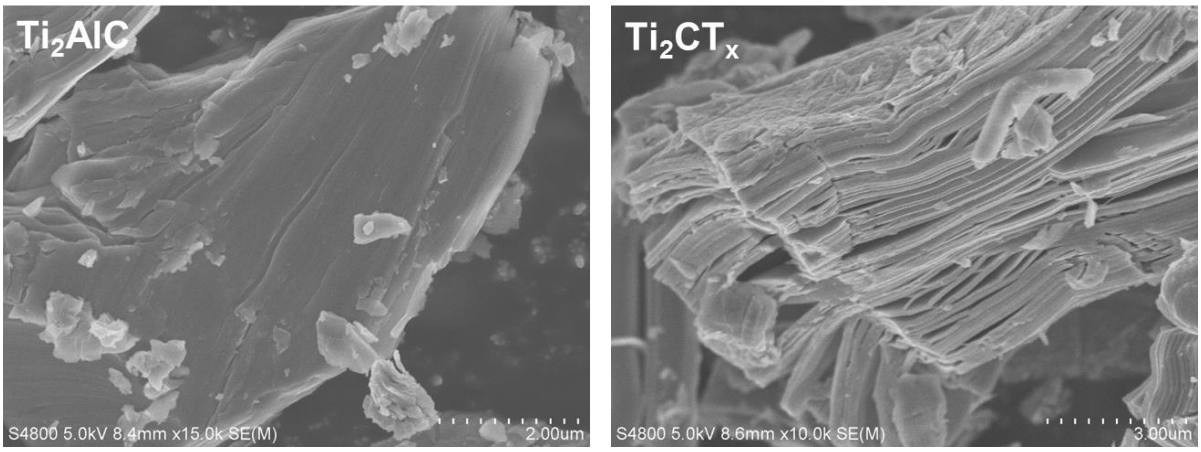

Figure S2. SEM images of Ti_2AlC and Ti_2CT_x. The particulate morphology of Ti_2AlC is transformed to stacked-nanosheet morphology after LiF/HCl treatment.

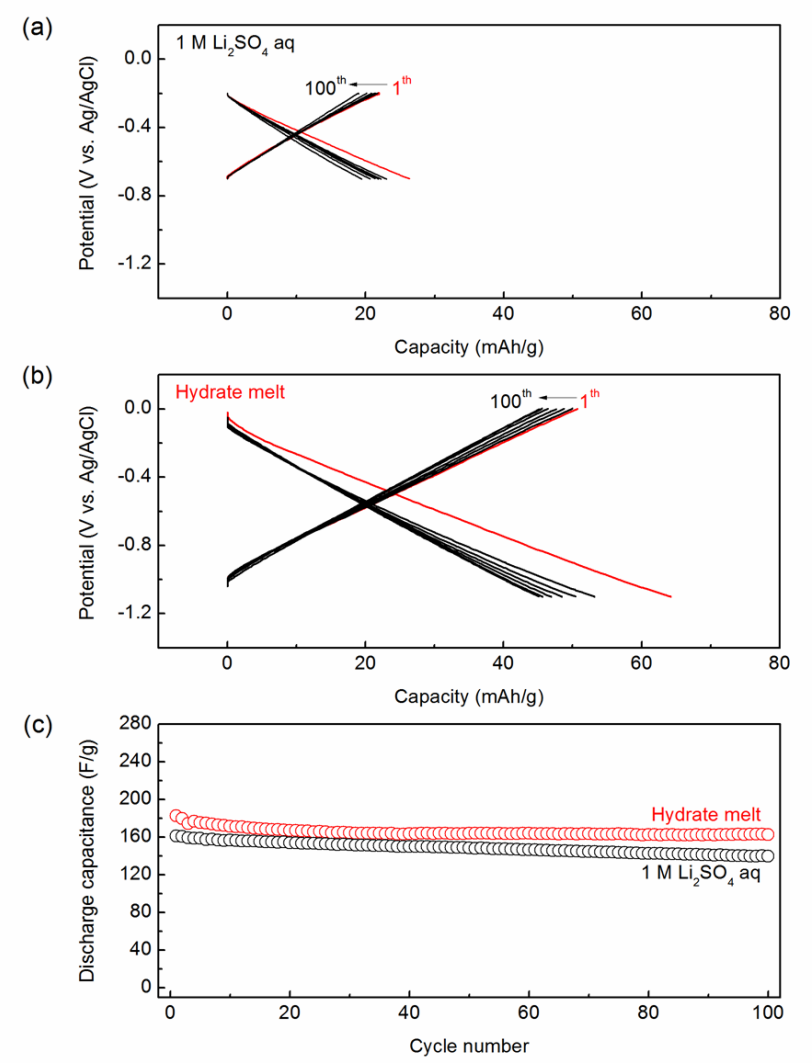

Figure S3. Galvanostatic charge/discharge curves of Ti_2CT_x with (a) 1.0 M Li_2SO_4 aqueous electrolyte and (b) a hydrate melt at a current rate of 0.2 A/g during 100 cycles. (c) Cycle stability (cycle number vs. discharge capacitance) of Ti_2CT_x with a 1.0 M Li_2SO_4 aqueous electrolyte and a hydrate-melt electrolyte at a specific current of 0.2 A/g. Discharge capacitance C (F/g) for linear charge-discharge curve is defined as $C = I\Delta t/m\Delta V$, where I is current intensity, Δt is discharge time, m is mass, and ΔV is voltage change of the electrode versus a reference electrode.

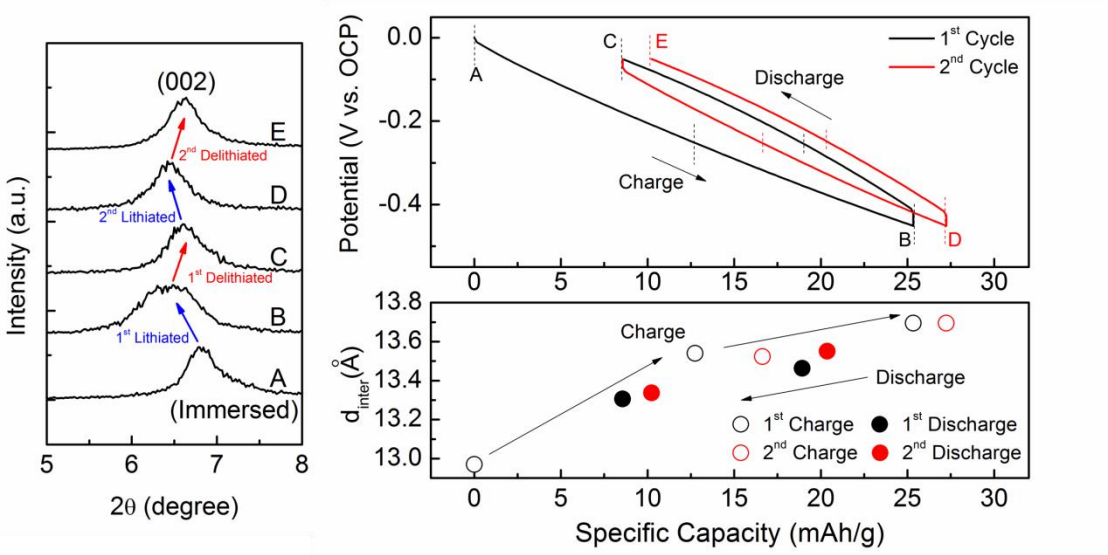

Figure S4. Ex-situ XRD patterns (Left), and the interlayer distance d_{inter} (right) of Ti_2CT_x upon charging/discharging with a 1.0 M Li_2SO_4 aqueous electrolyte during the first and second cycles.

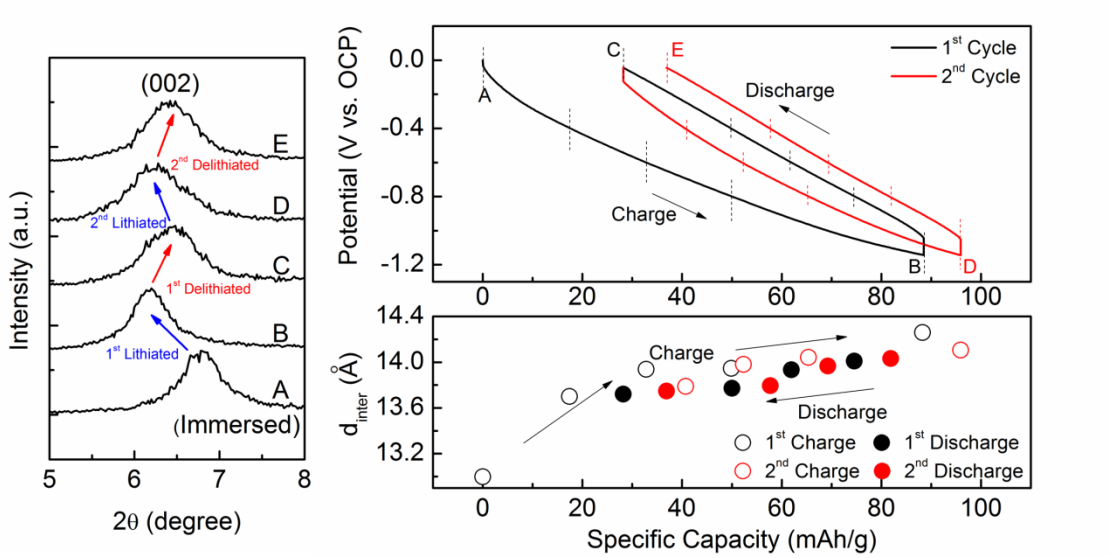

Figure S5. Ex-situ XRD patterns (Left), and the interlayer distance d_{inter} (right) of Ti_2CT_x upon charging/discharging with a hydrate-melt electrolyte during the first and second cycles.

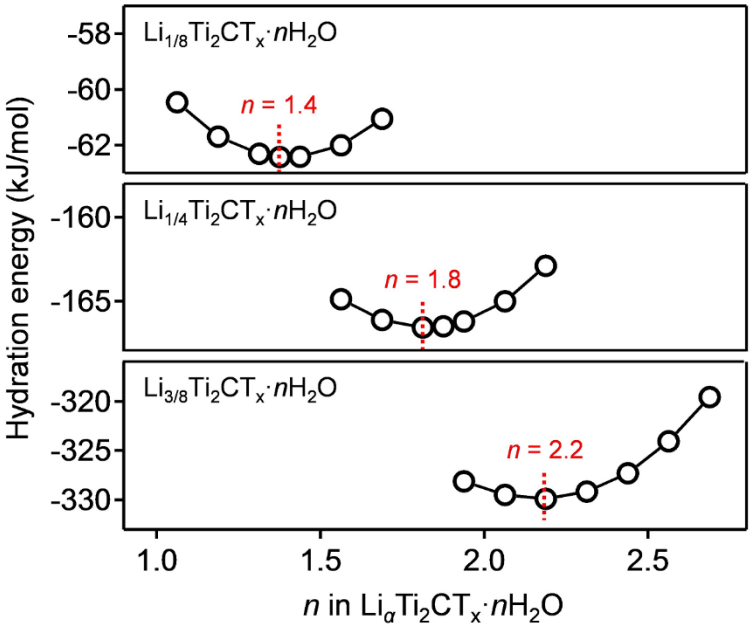

Figure S6. 3D-RISM optimization of hydration of Li^+ intercalated into Ti_2CT_x. Hydration energy of Li^+-intercalated MXenes, *i.e.*, $Li_\alpha Ti_2CT_x \cdot nH_2O$ (α = 1/8, 1/4, and 3/8) as a function of a hydration number n. During the optimization, the interlayer distance between Ti_2CT_x nanosheets was fixed at the experimental value in Figure S4. The optimal hydration was obtained at n = 1.4, 1.8, and 2.2 for α = 1/8, 1/4, and 3/8, respectively.

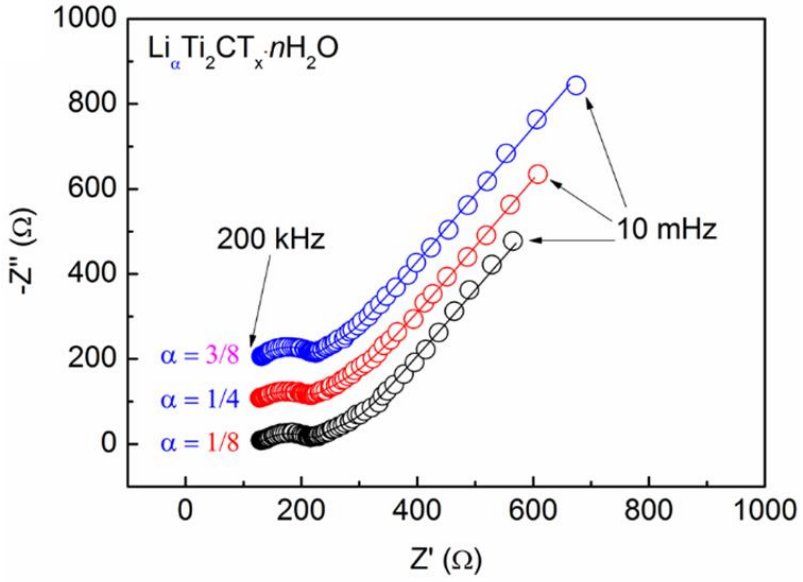

Figure S7. Nyquist plots for Ti_2CT_x with a hydrate-melt electrolyte at different states of charge (-0.5 V, -0.8 V, and -1.1 V vs. OCP) corresponding to $Li_\alpha Ti_2CT_x \cdot nH_2O$ (α = 1/8, 1/4, and 3/8). Empty circles: experimental, solid lines: fitting.

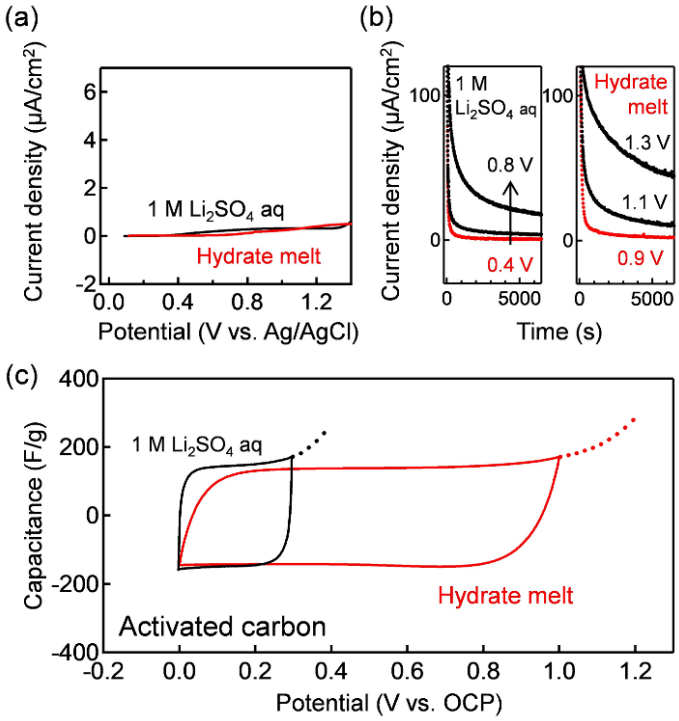

Figure S8. (a) Anodic linear sweep voltammetry of a 1 M Li_2SO_4 aqueous electrolyte and a hydrate-melt electrolyte with a Ti electrode at a sweep rate of 0.1 mV/s. (b) Chronoamperometry at various applied potentials vs. Ag/AgCl in a 1 M Li_2SO_4 aqueous electrolyte and a hydrate-melt electrolyte with activated carbon. Red lines indicate negligible steady-state leak current, which determines a cut-off voltage for each system. (c) Cyclic voltammetry curves of activated carbon with a 1.0 M Li_2SO_4 aqueous electrolyte (black line) and a hydrate-melt electrolyte (red line) at a scan rate of 0.5 mV/s. Open circuit potentials (OCP) are 0.15 V vs. Ag/AgCl for a 1.0 M Li_2SO_4 aqueous electrolyte and −0.05 V vs. Ag/AgCl for the hydrate-melt electrolyte, respectively. Dotted lines are linear sweep voltammetry curves for a cathodic scan exceeding a stable electrochemical window.

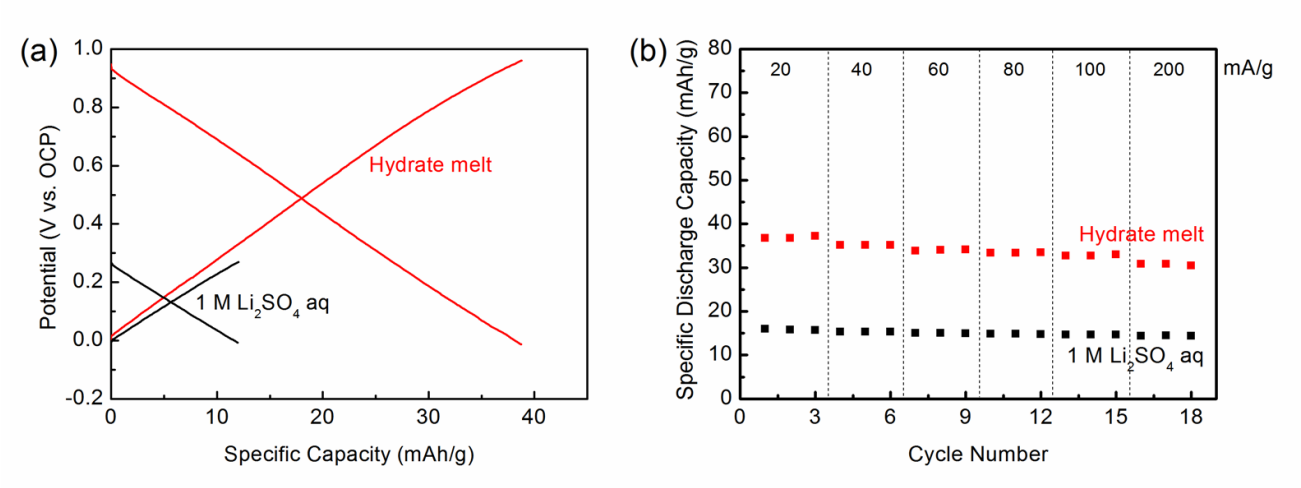

Figure S9. (a) Galvanostatic charge/discharge curves of activated carbon at a constant specific current of 30 mA/g with a 1.0 M Li_2SO_4 aqueous electrolyte (black lines), and with a hydrate-melt electrolyte (red lines). (b) Rate capability of activated carbon at various specific currents of 20-200 mA/g with a 1.0 M Li_2SO_4 aqueous electrolyte (black) and with a hydrate-melt electrolyte (red).

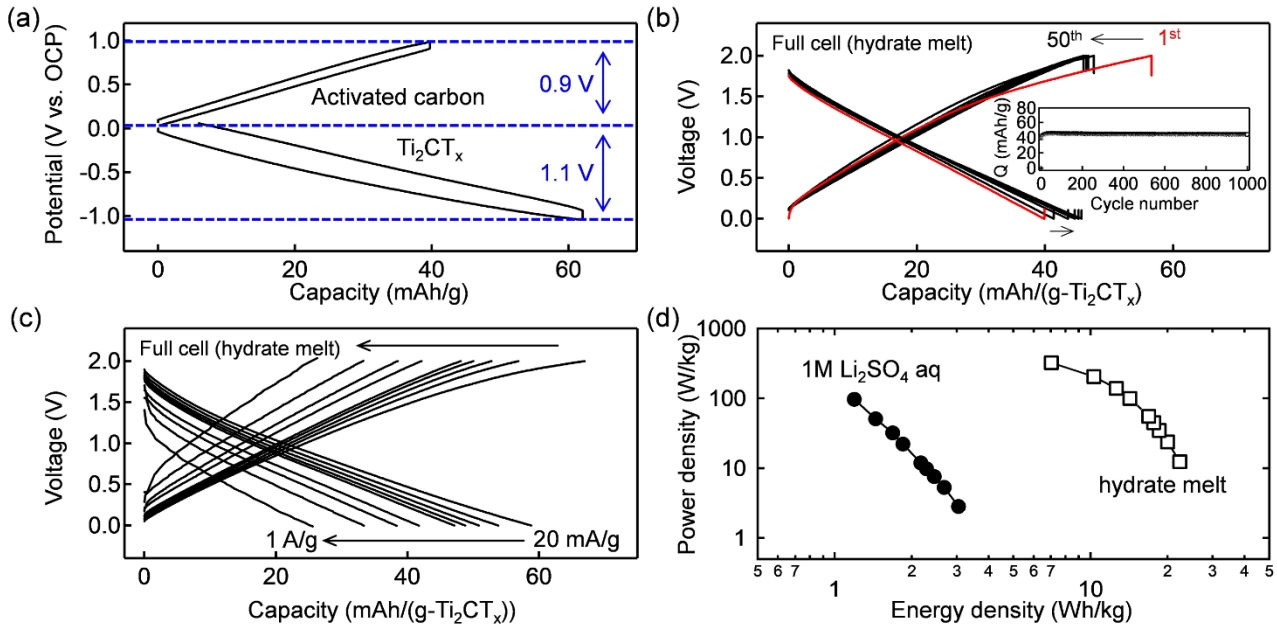

Figure S10. (a) Potential profiles of activated carbon and Ti_2CT_x in a hydrate-melt electrolyte at a specific current of 30 mA/g during the second cycle. (b) Voltage profiles of a capacity-balanced full-cell consisting of a Ti_2CT_x negative electrode and an activated carbon positive electrode with a hydrate-melt electrolyte. Cell was cycled at a specific current of 100 mA/g in the voltage range of 2.0 – 0.0 V. Inset shows the cycle stability during 1000 cycles. (c) Rate capability with various specific currents. All the capacity values are based on the weight of Ti_2CT_x. (d) Ragone plots of the Ti_2CT_x/AC full-cell with a hydrate-melt electrolyte (empty squares) and a 1.0 M Li_2SO_4 aqueous electrolyte (filled circles). Energy and power densities are calculated based on the total weight of the positive and negative electrodes.

Table S1. Elemental analysis results of Ti_2CT_x before and after drying at 200˚C.

	C/wt%	H/wt%	F/wt%	Cl/wt%
Exp. Ti_2CT_x before drying	6.15	1.34	6.54	7.94
Cal. for $Ti_2C(OH)O_{0.3}F_{0.6}Cl_{0.4}\cdot 0.4H_2O$	7.39	1.11	7.02	8.74
Exp. for Ti_2CT_x after drying	6.98	0.58	6.76	9.01
Cal. for $Ti_2C(OH)O_{0.3}F_{0.6}Cl_{0.4}$	7.74	0.64	7.34	9.14

Table S2. Energy dispersive X-ray spectroscopy analysis of Ti_2AlC and Ti_2CT_x.

	Ti atomic%	C atomic%	Al atomic%	O atomic%	F atomic%	Cl atomic%
Ti_2AlC	52.99	26.45	20.56	-	-	-
Ti_2CT_x	42.49	22.91	0.93	17.04	8.46	8.18